

**Consistent Parameter Set for an Ensemble Monte Carlo Simulator Used for  
Describing Experimental Low-Field and High-Field  
Transport Parameters of 4H-SiC**

N. Ashraf, D. Vasileska and D.K. Ferry

*Department of Electrical Engineering, Ira A. Fulton School of Engineering  
Arizona State University, Tempe, AZ, 85287-5706, USA*

**Abstract**

A consistent parameter set is presented for Ensemble Monte Carlo simulation that simultaneously reproduces the experimental low-field and high-field characteristic transport parameters of 4H SiC.

## 1. Introduction

The physical properties of silicon carbide, such as large bandgap (3-3.2 eV), high avalanche breakdown field (2.5-3 MV/cm) and high thermal conductivity (4-5 W/cm-K) make SiC an attractive candidate for high voltage, high temperature and high power device applications [1,2]. One of the most significant advantages of SiC is the ability to grow a stable thermal oxide, enabling fabrication of MOS-based device structures. While high-voltage power MOSFETs [3,4,5,6] have already been demonstrated in SiC, further development is challenged by poor inversion layer mobility, especially in the 4H polytype. The full potential of SiC [7] is not yet utilized because the performance of the SiC MOS-based devices is limited by the resistance of the MOS channel and not by the high-resistivity blocking layer. 4H-SiC is favored over 6H-SiC because of the higher and more isotropic bulk mobility, which translates to lower on-resistance in power devices; however for identical processing conditions, channel mobilities are significantly lower in 4H-SiC than 6H-SiC [8,9,10].

The above discussion suggests that proper modeling of the inversion layer mobility of the 4H-SiC is of significant experimental and theoretical importance. This, in turn, requires the knowledge of the bulk mobility because one can understand the interplay of various scattering mechanisms and parameters that need to be used for describing acoustic, polar optical and intervalley phonon scattering mechanisms properly. In this brief we report on a unique set of parameters that has been used within an Ensemble Monte Carlo (EMC) simulations scheme that simultaneously reproduces the doping dependence of the low-field mobility, temperature dependence of the mobility and the saturation drift velocity variation vs. electric field. Note that the experimental data are taken from several independent sources which proves the consistency of our set of parameters.

## 2. Theoretical Model

4H-SiC is a wurtzite material and has hexagonal Brillouin Zone (BZ). The labeling of the symmetry points and the three symmetry lines out from the  $\Gamma$  point in the relevant cubic and hexagonal BZs are shown in Figure 1. The resulting band structure for the 4H-SiC bands within a few eV from the band gap are presented in the top panel of Figure 2 [11].

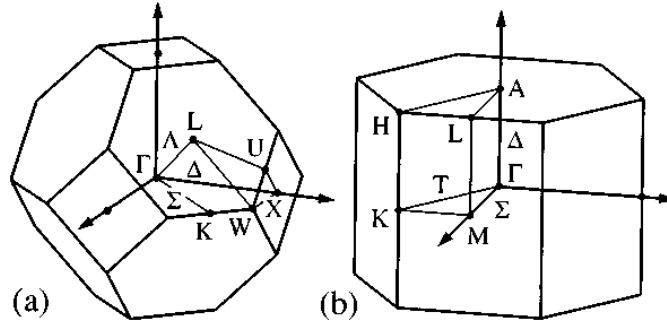


Figure 1. Brillouin zones of the face-centered cubic and hexagonal structures.

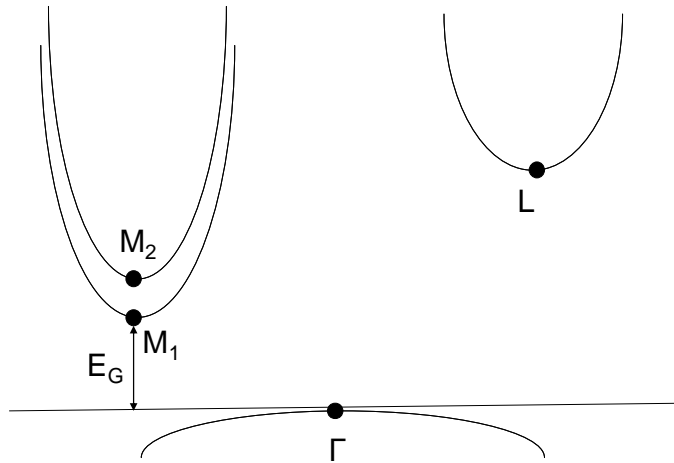
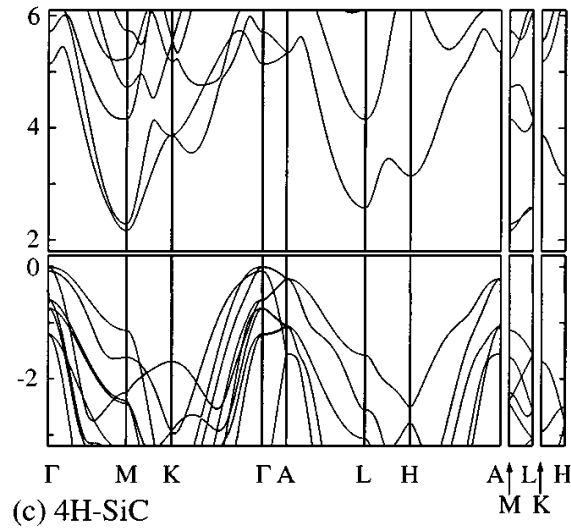


Figure 2. Top panel: Energy bands in the vicinity of the energy gap for 4H-SiC. The energies are referenced to the top of the valence band and the band gap has been removed. Bottom panel: Model band-structure for the conduction band used in our Ensemble Monte Carlo model.

The electron band structure of 4H-SiC consists of two bands centered at point  $M_1$  and  $M_2$  of the Brillouin zone and a third lowest band centered at the L point. In energy space, bands 2 and 3 are above band 1 with energy separations given in Table 1. The nonparabolicity parameters of the bands are also listed in Table 1. In our EMC code model we have taken the  $3M_1$ ,  $3M_2$  and the 6L conduction band valleys as model bandstructure. This model band-structure is schematically shown in the bottom panel of Figure 2. As already noted, we consider Coulomb, acoustic phonon, polar optical phonon and intervalley scattering. The parameters used for describing the various scattering mechanisms included in the theoretical model are summarized in Table 2. Details of the EMC code used in this study can be found elsewhere [12].

**Table 1. Model band-structure used in the Monte Carlo simulation of bulk 4H-SiC**

Parameters of Electron bands	$M_1$	$M_2$	L
Band	1	2	3
Perpendicular effective mass	0.42	0.35	0.66
Parallel effective mass	0.28	0.71	0.15
Nonparabolicity constant ( $eV^{-1}$ )	0.323	0.45	0.2
Intervalley energy separation ( eV )	0	0.122	0.7

**Table 2. 4H-SiC material and scattering parameters**

Mass density	$3.2 \times 10^3 \text{ kg/m}^3$
Sound velocity	$1.373 \times 10^3 \text{ m/s}$
Static dielectric constant	9.7
High-frequency dielectric constant	6.5
Acoustic deformation potential	1.5 eV
Polar optical phonon energy	0.120 eV
Intervalley and interband electron coupling	$7 \times 10^{10} \text{ eV/m}$
Intervalley and interband phonon energy	0.0854 eV

### 3. Simulation Results

Drift velocities in the y direction under the application of electric field are extracted by EMC simulation for two different electric field biases. The velocity, as it passes through the transient phase, shows overshoot due to finite momentum relaxation time redistribution effect

within this transient zone. The velocity eventually reaches steady state after a time of approximately 1 ps. Figure 3 shows the characteristic of the time evolution of the drift velocity.

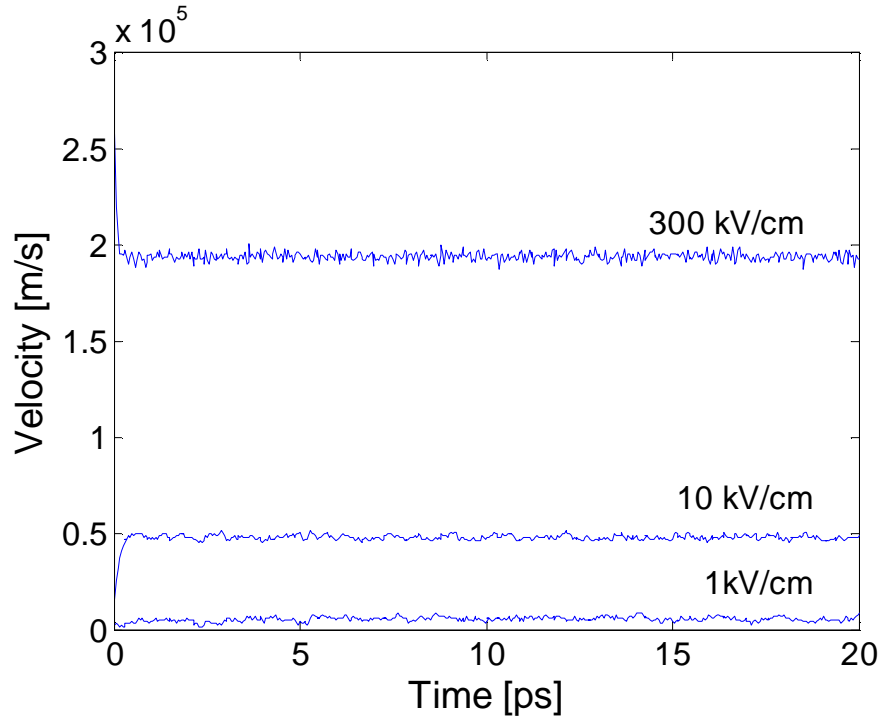


Figure 3: Transient and steady state drift velocity for the application of (i) 1 kV/cm and (ii) 10 kV/cm and (iii) 300 kV/cm electric fields, respectively.

Results are also extracted to probe into high field transport characteristics of bulk 4H-SiC. EMC simulation run was performed to simulate drift velocity along the y-direction as a function of electric field applied along the y axis. The bulk doping selected is  $10^{22} \text{ m}^{-3}$  to enable comparison with experimentally measured values of velocity for this doping [13]. The MC simulation shows linear increase of velocity for low applied field resulting in presumably near constant mobility, a feature known for low applied electric fields. As the electric field is increased, the velocity trend tends to increase slowly to its maximum peak around  $1.9 \times 10^7 \text{ cm/s}$  at an electric field of  $3 \times 10^5 \text{ V/cm}$ . After this field the velocity drops as intervalley transition to  $M_2$  and L valley takes place whose effective masses are higher than  $M_1$  valley. The EMC simulated velocity profile fits very well with experimental values shown with solid circles. Figure 4 depicts this characteristic.

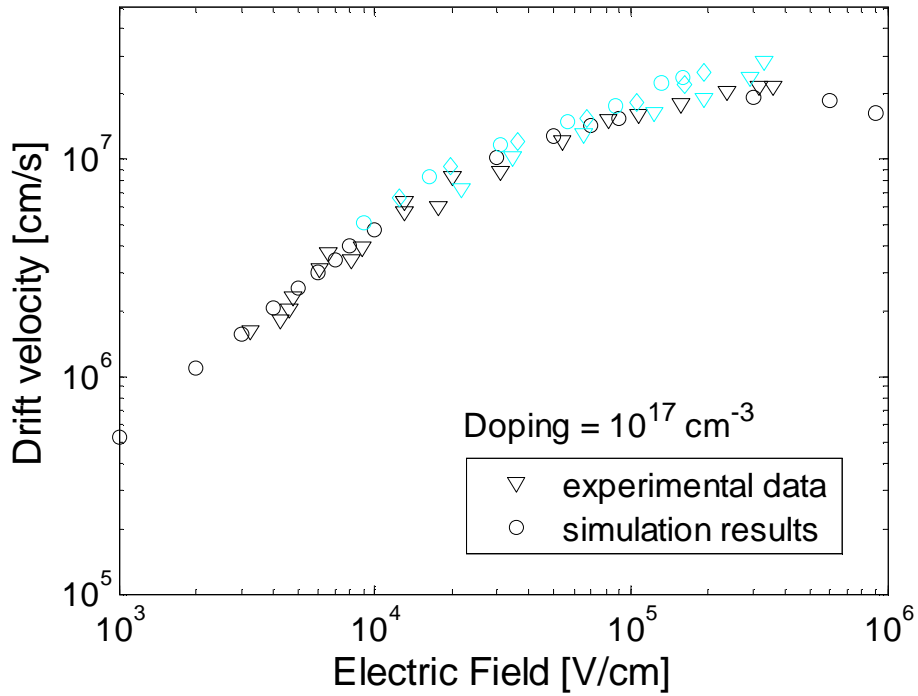


Figure 4: EMC code simulated velocity field characteristics fitted with experimentally available sample data. The cyan circles, diamonds and triangles are the simulation results from Ref. [7] for three different sets of parameters values.

The Ensemble Monte Carlo simulation, used to extract low field mobility as a function of doping, generates very good profile with the mobility being more or less flat in the doping region  $10^{20}$  -  $10^{21} \text{ m}^{-3}$  and sharply falling between  $10^{21}$  -  $10^{22} \text{ m}^{-3}$  before flattening out near  $10^{23}$  -  $10^{24} \text{ m}^{-3}$ . This is typical for a low to moderate to highly degenerate doping conditions. The correlation with experimentally available sample data [12] is very good and most of the solid circles cluster around the simulated profile curve. This behavior is shown in Figure 5.

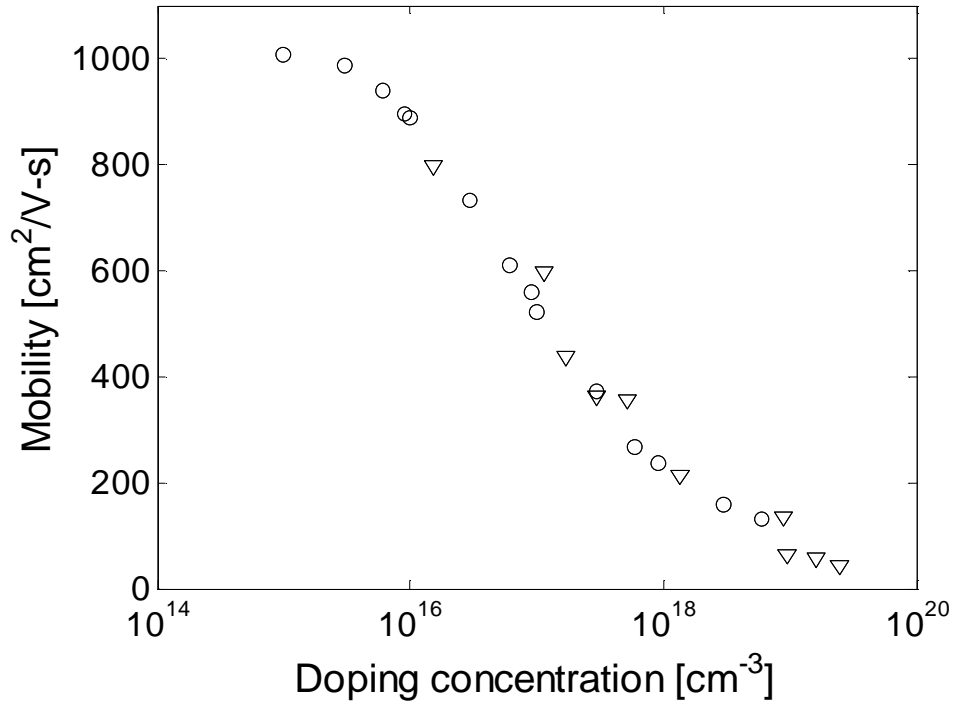


Figure 5: MC simulated mobility as a function of doping. Also shown are experimental data from Ref. [12]. Open circles are EMC simulation results and open triangles are experimental data.

Low field mobility dependence on temperature has also been investigated with our MC code and the profile is typical as the mobility gradually decreases from low to slightly above room temperature value and then plummets for high enough temperature value. Interaction resulting from acoustic phonons causes this mobility decrease which is explained in conventional theory. Comparison was made with experimentally available sample data [12] referenced to a bulk doping of  $6 \times 10^{22} \text{ m}^{-3}$  at which ratio of room temperature mobility value measured experimentally to MC simulated mobility value normalizes to unity. The agreement is quite good with the experimental values. These results are shown in Figure 6.

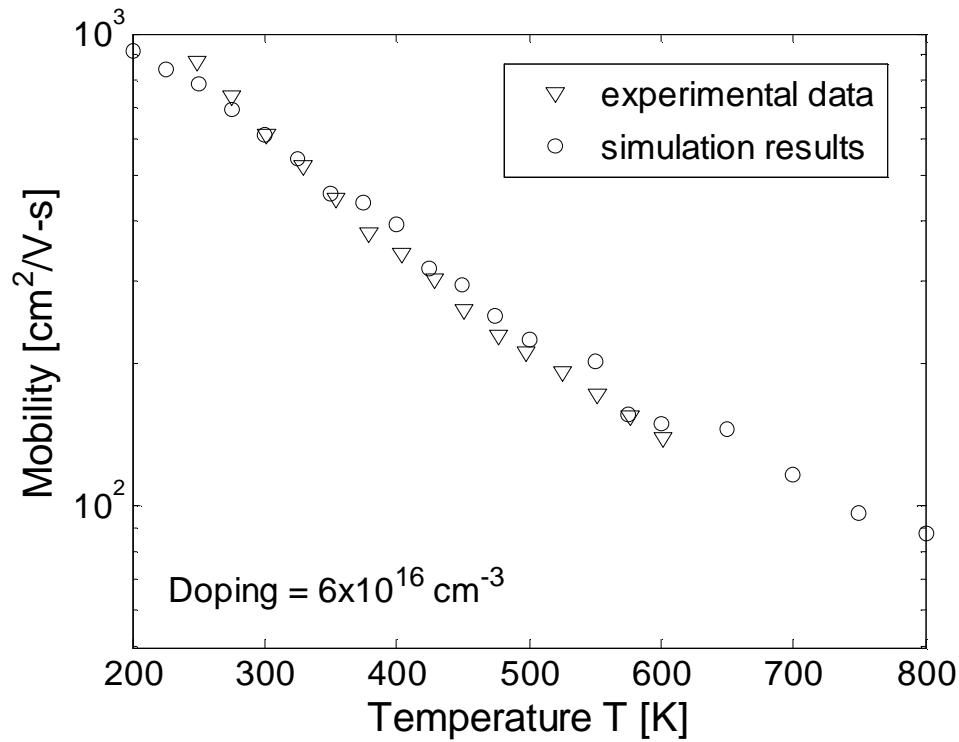


Figure 6: Low field mobility dependence on temperature and its comparison with experimental data.

### Conclusion

A robust and efficient Ensemble Monte Carlo code has been developed which can be used as a tool to simulate the bulk transport properties of 4H-SiC devices. The bulk transport parameters such as drift velocity and mobility values exhibit good correlation with the industry or laboratory measured experimental data points. A set of scattering parameters are also generated by this MC code giving further insight about transport processes involved in intravalley and intervalley transitions and other processes commonly cited in literature. Current research analysis and report on this issue will serve as a valuable guideline to extract a generic set of scattering parameters listed in Table II to eventually emulate and fit other experimental or device simulation based sample data points. These set of parametric values along with the EMC code will be very helpful to practicing engineers, researchers and industry staffs who are involved with device analysis of 4H-SiC based device manufacturing .

## References

---

- <sup>1</sup> C.E. Weitzel, J.W. Palmour, C.H. Carter, Jr., K. Moore, K.J. Nordquist, S. Allen, C. Them, and M. Bhatnagar, *IEEE Trans. Electron Dev.* **43**, 1732 (1996).
- <sup>2</sup> T.P. Chow, N. Ramungul, and M. Ghezzi, *MRS Fall Meeting* (Boston, MA: 1997).
- <sup>3</sup> J.N. Shenoy, J.A. Cooper, Jr., and M.R. Melloch, *IEEE Electron Dev. Lett.* **18**, 93 (1997).
- <sup>4</sup> A.K. Agarwal, J.B. Casady, L.B. Rowland, W.F. Valek, M.H. White, and C.D. Brandt, *IEEE Electron Dev. Lett.* **18**, 586 (1997).
- <sup>5</sup> J. Spitz, M.R. Melloch, J.A. Cooper, Jr., and M.A. Capano, *IEEE Electron Dev. Lett.* **19**, 100 (1998).
- <sup>6</sup> K. Chatty, S. Banerjee, T.P. Chow, and R.J. Gutmann, *IEEE Electron Dev. Lett.* **21**, 356 (2000).
- <sup>7</sup> D. K. Ferry, *Phys. Rev. B* **12**, 2361 (1975).
- <sup>8</sup> R. Schorner, P. Friedrichs, D. Peters, and D. Stephani, *IEEE Electron Dev. Lett.* **20**, 241 (1999).
- <sup>9</sup> N.S. Saks and A.X. Agarwal, *Appl. Phys. Lett.* **77**, 3281 (2000).
- <sup>10</sup> M.K. Das, B.S. Um, and J.A. Cooper, Jr., *Mater. Sci. Forum* **338-342**, 1069 (2000).
- <sup>11</sup> C. Persson and U. Lindefelt, *J. Appl. Phys.* **82**, 5496 (1997).
- <sup>12</sup> D. Vasileska and S. M. Goodnick, *Computational Electronics*, Morgan and Claypool, 2006.
- <sup>13</sup> M. Roschke and F. Schwierz, *IEEE Trans. Electron Dev.* **48**, 1442 (2001), and the references therein.